

NUMERICAL SOLUTION OF SECOND ORDER ONE-DIMENSIONAL LINEAR HYPERBOLIC EQUATION USING TRIGONOMETRIC WAVELETS

MAHMOOD JOKAR AND MEHRDAD LAKESTANI

A numerical technique is presented for the solution of second order one dimensional linear hyperbolic equation. This method uses the trigonometric wavelets. The method consists of expanding the required approximate solution as the elements of trigonometric wavelets. Using the operational matrix of derivative, we reduce the problem to a set of algebraic linear equations. Some numerical example is included to demonstrate the validity and applicability of the technique. The method produces very accurate results. An estimation of error bound for this method is presented and it is shown that in this method the matrix of coefficients is a sparse matrix.

Keywords: telegraph equation, trigonometric wavelets, hermite interpolation, operational matrix of derivative

Classification: 65T60, 65T40, 65L60, 35L20

1. INTRODUCTION

Consider the second order one dimensional linear hyperbolic equation

$$\mathcal{A}u = f, \tag{1}$$

where \mathcal{A} is an linear partial differential operator as

$$\begin{aligned} \mathcal{A}u &= (\mathcal{D}_t - \mathcal{D}_x + \beta^2 \mathcal{I})u \\ &= \frac{\partial^2 u}{\partial t^2}(x, t) + 2\alpha \frac{\partial u}{\partial t}(x, t) - \frac{\partial^2 u}{\partial x^2}(x, t) + \beta^2 u(x, t) = f(x, t) \end{aligned} \tag{2}$$

$(x, t) \in [0, 2\pi] \times [0, 2\pi], \alpha > \beta \geq 0$

where

$$\begin{aligned} \mathcal{D}_t u(x, t) &= \left(\frac{\partial^2}{\partial t^2} + 2\alpha \frac{\partial}{\partial t} \right) u(x, t), \\ \mathcal{D}_x u(x, t) &= \frac{\partial^2}{\partial x^2} u(x, t), \\ \mathcal{I}u(x, t) &= u(x, t), \end{aligned}$$

with initial conditions

$$u(x, 0) = g_1(x), \quad (3)$$

$$\frac{\partial u}{\partial t}(x, 0) = g_2(x), \quad (4)$$

and boundary conditions

$$u(0, t) = h_1(t), \quad t \geq 0, \quad (5)$$

$$u(2\pi, t) = h_2(t), \quad t \geq 0. \quad (6)$$

The hyperbolic partial differential equations model the vibrations of structures (e.g., buildings, beams, and machines) and are the basis for fundamental equations of atomic physics.

In recent years, much attention has been given in the literature to the development, analysis, and implementation of stable methods for the numerical solution of second-order hyperbolic equations, see, for example [5, 19, 27]. These methods are conditionally stable. Mohanty [20, 21] made investigations on the one-space-dimensional hyperbolic equations. In [20], Mohanty carried over a new technique to solve the linear one-space-dimensional hyperbolic equation (1), which is unconditionally stable and is of second-order accurate in both time and space components. Also this author proposed in [21] a three level implicit unconditionally stable difference scheme [16] of second-order accurate in both time and space variables for the solution of (1.1) with variable coefficients that fictitious points are not needed at each time step along the boundary. Authors of [22] presented a high-order accurate method for solving one-space-dimensional linear hyperbolic equation. A compact finite difference approximation [6] of fourth order for discretizing spatial derivative of linear hyperbolic equation and collocation method for the time component are used in their work. The main property of the approach in [22] additional to its high-order accuracy due to the fourth-order discretization of spatial derivative, is its unconditionally stability. In their technique, the solution is approximated by a polynomial at each grid point that its coefficients are determined by solving a linear system of equations [7]. A numerical scheme is developed in [8] to solve the one-dimensional hyperbolic telegraph equation using the collocation points [7] and approximating the solution using thin plate splines radial basis function. Also several test problems are given and the results of numerical experiments are compared with analytical solutions to confirm the good accuracy of the presented scheme. A Chebychev Cardinal functions method presented in [9] to solve telegraph equation numerically. In [14] was given an interpolating scaling function method for numerical solution of telegraph equation.

The wavelet approach has been proved already as an efficient tool to analyze functions [3]. The trigonometric Hermite interpolation enables a completely explicit description of the corresponding decomposition and reconstruction coefficients by means of some circular matrices. Starting from consideration on \mathbb{R}^n there are also well-known results on bounded intervals and in the periodic case. In particular, in the periodic case a wavelet analysis by trigonometric polynomials is obtained for the first time by C. K. Chui, H. N. Mhaskar [2].

In the present paper we apply the Hermite interpolation by trigonometric wavelets, to solve second order one dimensional linear hyperbolic equation of the form 1. The purpose of the present paper is to develop a trigonometric Hermite wavelet Galerkin

approximation for the second order one dimensional linear hyperbolic telegraph equation. Finally, the convergence analysis of this wavelet Galerkin method for the telegraph equation 1 is developed. Considering this basis being trigonometric polynomial, our method is essentially a spectral method.

The outline of this paper is as follows. In Section 2, we describe the trigonometric scaling and wavelet functions on $[0, 2\pi]$ and introduce the operational matrix of the derivative for these functions. In Section 3, the proposed method is used to approximate the solution of the problem. As a result a set of algebraic equations is formed and a solution of the considered problem is introduced. In Section 4, we discuss the convergence analysis of the trigonometric Hermite wavelet method in this paper. In Section 5, we report our computational results and demonstrate the accuracy of the proposed numerical scheme by presenting numerical examples. Section 6 ends this paper with a brief conclusion.

2. TRIGONOMETRIC SCALING AND WAVELET FUNCTION ON $[0, 2\pi]$

In this section, we will give a brief introduction of Quak’s work on the construction of Hermite interpolatory trigonometric wavelets and their basic properties [24]. Throughout this study we denote by $L^2_{2\pi}$ the set of 2π -periodic square-integrable functions f as

$$L^2_{2\pi} = \left\{ f : \int_0^{2\pi} |f(x)|^2 dx < \infty, f(x) = f(x + 2\pi), x \in \mathbb{R} \right\}.$$

Let T_n denote the linear space of trigonometric polynomials with degree not exceeding n . For all $n \in \mathbb{N}$, the Dirichlet kernel $D_n(x)$ and its conjugate kernel $\tilde{D}_n(x)$ are defined as [24, 26]

$$D_n(x) = \frac{1}{2} + \sum_{k=1}^n \cos kx, \tag{7}$$

$$\tilde{D}_n(x) = \sum_{k=1}^n \sin kx. \tag{8}$$

Let $x_{j,n} = \frac{n\pi}{2^j}$, $j \in \mathbb{N}_0$, $n = 0, 1, \dots, 2^{j+1} - 1$, where $\mathbb{N}_0 = \mathbb{N} \cup \{0\}$.

Definition 2.1. The scaling function spaces are defined by $V_j = span\{\phi_{j,n}^0, \phi_{j,n}^1, n = 0, \dots, 2^{j+1} - 1\}$, where

$$\phi_{j,0}^0(x) = \frac{1}{2^{2j+1}} \sum_{k=0}^{2^{j+1}-1} D_k(x), \quad \phi_{j,0}^1(x) = \frac{1}{2^{2j+1}} \left(\tilde{D}_{2^{j+1}-1}(x) + \frac{1}{2} \sin(2^{j+1}x) \right),$$

and $\phi_{j,n}^s(x) = \phi_{j,0}^s(x - x_{j,n})$, $s = 0, 1$, $n = 0, 1, \dots, 2^{j+1} - 1$.

Theorem 2.2. (see Chui [24]) For all $j \in \mathbb{N}_0$, the following interpolation properties hold for each $k, n = 0, 1, \dots, 2^{j+1} - 1$,

$$\phi_{j,n}^0(x_{j,k}) = \delta_{k,n}, \quad (\phi_{j,n}^0)'(x_{j,k}) = 0, \tag{9}$$

$$\phi_{j,n}^1(x_{j,k}) = 0, \quad (\phi_{j,n}^1)'(x_{j,k}) = \delta_{k,n}, \tag{10}$$

where $\delta_{k,n}$ is the Kronecker delta.

Given $j \in \mathbb{N}_0$, the space V_j is defined by $V_j = \text{span}\{1, \cos x, \dots, \cos(2^{j+1} - 1)x, \sin x, \dots, \sin 2^{j+1}x\}$.

Definition 2.3. For $j \in \mathbb{N}_0$, the wavelet spaces are defined by $W_j = \text{span}\{\psi_{j,n}^0, \psi_{j,n}^1, n = 0, \dots, 2^{j+1} - 1\}$, where

$$\psi_{j,0}^0(x) = \frac{1}{2^{j+1}} \cos(2^{j+1}x) + \frac{1}{3 \cdot 2^{2j+1}} \sum_{l=2^{j+1}+1}^{2^{j+2}-1} (3 \cdot 2^{j+1} - l) \cos(lx), \tag{11}$$

$$\psi_{j,0}^1(x) = \frac{1}{3 \cdot 2^{2j+1}} \sum_{l=2^{j+1}+1}^{2^{j+2}-1} \sin(lx) + \frac{1}{2^{2j+3}} \sin(2^{j+2}x), \tag{12}$$

and $\psi_{j,n}^s(x) = \psi_{j,0}^s(x - x_{j,n})$, $s = 0, 1$, $n = 0, 1, \dots, 2^{j+1} - 1$.

2.1. The function approximation

For any $j \in \mathbb{N}_0$, the operator P_j mapping any real-valued differentiable 2π -periodic function f into the space V_j is defined as

$$P_j f(x) = \sum_{k=0}^{2^{j+1}-1} [a_k \phi_{j,k}^0(x) + b_k \phi_{j,k}^1(x)] = \Phi^T F, \tag{13}$$

where $P_j f \in V_j \subset T_{2^{j+1}}$, $F = [a_0, \dots, a_{2^{j+1}-1}, b_0, \dots, b_{2^{j+1}-1}]^T$,

$$\Phi = [\phi_{j,0}^0, \dots, \phi_{j,2^{j+1}-1}^0, \phi_{j,0}^1, \dots, \phi_{j,2^{j+1}-1}^1]^T, \tag{14}$$

are vectors with dimensions $2^{j+2} \times 1$, and

$$a_k = f(x_{j,k}), \quad b_k = f'(x_{j,k}), \quad k = 0, 1, \dots, 2^{j+1} - 1. \tag{15}$$

Furthermore, It follows that

$$P_j f(x) = \sum_{k=0}^1 [a_k \phi_{1,k}^0(x) + b_k \phi_{1,k}^1(x)] + \sum_{l=0}^{j-1} \sum_{k=0}^{2^{l+1}-1} [c_{l,k} \psi_{l,k}^0(x) + d_{l,k} \psi_{l,k}^1(x)] = \Psi^T \hat{F}, \tag{16}$$

where $\phi_{1,k}^s(x)$ and $\psi_{j,k}^s$ are scaling and wavelets functions, respectively, and \hat{F} and Ψ are $2^{j+2} \times 1$ vectors given by $\hat{F} = [a_0, a_1, b_0, b_1, c_{0,0}, \dots, c_{j,2^j-1}, d_{0,0}, \dots, d_{j,2^j-1}]^T$, and

$$\Psi = [\phi_{1,0}^0, \phi_{1,1}^0, \phi_{1,0}^1, \phi_{1,1}^1, \psi_{0,0}^0, \dots, \psi_{j,2^j-1}^0, \psi_{0,0}^1, \dots, \psi_{j,2^j-1}^1]^T, \tag{17}$$

where

$$\hat{F} = G^T F, \tag{18}$$

and G is the $2^{J+2} \times 2^{J+2}$ transform matrix between vectors Ψ and Φ , as [15]

$$\Phi = G\Psi. \tag{19}$$

The projection of two-dimensional smooth function $k(x, t)$ in the space $V_J \otimes V_J$, is as

$$P_J k(x, t) = \Phi^T(x) K \Phi(t), \tag{20}$$

where K is a block matrix with dimension $2^{J+2} \times 2^{J+2}$ as

$$K = \begin{bmatrix} k_1 & k_2 \\ k_3 & k_4 \end{bmatrix}, \tag{21}$$

and

$$k_1(i, l) = k(x_{J,i}, x_{J,l}), \quad k_2(i, l) = \frac{\partial k(x, t)}{\partial t} \Big|_{(x_{J,i}, x_{J,l})},$$

$$k_3(i, l) = \frac{\partial k(x, t)}{\partial x} \Big|_{(x_{J,i}, x_{J,l})}, \quad k_4(i, l) = \frac{\partial^2 k(x, t)}{\partial x \partial t} \Big|_{(x_{J,i}, x_{J,l})},$$

for $i, l = 0, 1, \dots, 2^{J+1} - 1$. Also using Eq. (19) we get

$$P_J k(x, t) = \Psi^T(x) G^T K G \Psi(t).$$

2.2. The operational matrix of derivative

The differentiation of vector Φ and Ψ in (14) and (17) can be expressed as [12, 13, 14]

$$\Phi' = D_\phi \Phi, \quad \Psi' = D_\psi \Psi, \tag{22}$$

where D_ϕ and D_ψ are $2^{J+2} \times 2^{J+2}$ operational matrices of derivative for trigonometric scaling and wavelet functions, respectively. The matrix D_ϕ was represented in [15] as a block matrix as

$$D_\phi = \begin{bmatrix} A^0 & B^0 \\ A^1 & B^1 \end{bmatrix}, \tag{23}$$

where A^0 is a $2^{j+1} \times 2^{j+1}$ zero matrix, A^1 is a $2^{j+1} \times 2^{j+1}$ identity matrix,

$$B^0 = (b_{k,n}^0) = \begin{cases} \frac{1}{2} \frac{\cos((n-k)2\pi)}{\sin^2(\frac{n-k}{2^{j+1}}\pi)}, & k \neq n, \\ -\frac{1}{2^{2j+1}} \sum_{p=0}^{2^{j+1}-1} \frac{p(p+1)(2p+1)}{6}, & k = n, \end{cases}$$

and

$$B^1 = (b_{k,n}^1) = \begin{cases} -\cot \frac{(n-k)\pi}{2^{j+1}}, & k \neq n, \\ 0, & k = n, \end{cases}$$

for $k, n = 0, 1, \dots, 2^{j+1} - 1$. Using Eqs. (19), and (23) we get

$$\Psi' = G^{-1} \Phi' = G^{-1} D_\phi \Phi = G^{-1} D_\phi G \Psi.$$

So using Eq. (22), the matrix D_ψ can be obtained as

$$D_\psi = G^{-1} D_\phi G. \tag{24}$$

3. DESCRIPTION OF NUMERICAL METHOD

Consider the second order one dimensional linear hyperbolic equation (1). Using Eq. (20) we can approximate $u(x, t)$ as

$$u(x, t) = \Phi^T(t)U\Phi(x), \tag{25}$$

where U is a $2^{J+2} \times 2^{J+2}$ unknown matrix and should be found. Now using Eqs. (22) and (25) we can write

$$u_t(x, t) = \Phi'(t)U\Phi(x) = \Phi(t)D_\phi^T U\Phi(x), \tag{26}$$

$$u_{tt}(x, t) = \Phi(t)(D_\phi^2)^T U\Phi(x), \tag{27}$$

and

$$u_{xx}(x, t) = \Phi(t)UD_\phi^2\Phi(x). \tag{28}$$

Also using Eq. (20), the function $f(x, t)$ in Eq. (1) can be approximated as

$$f(x, t) = \Phi^T(t)K\Phi(x), \tag{29}$$

where K is a $2^{J+2} \times 2^{J+2}$ matrix as (21) with submatrices

$$\begin{aligned} k_1(i, l) &= f(x_{J,i}, x_{J,l}), \\ k_2(i, l) &= \left. \frac{\partial f(x, t)}{\partial t} \right|_{(x_{J,i}, x_{J,l})}, \\ k_3(i, l) &= \left. \frac{\partial f(x, t)}{\partial x} \right|_{(x_{J,i}, x_{J,l})}, \\ k_4(i, l) &= \left. \frac{\partial^2 f(x, t)}{\partial x \partial t} \right|_{(x_{J,i}, x_{J,l})}. \end{aligned}$$

Using Eqs.(25) – (29) in Eq.(1) we get

$$\begin{aligned} &\Phi^T(t)(D_\phi^2)^T U\Phi(x) + 2\alpha\Phi^T(t)D_\phi^T U\Phi(x) - \Phi^T(t)UD_\phi^2\Phi(x) \\ &+ \beta^2\Phi^T(t)U\Phi(x) = \Phi^T(t)K\Phi(x), \end{aligned} \tag{30}$$

or

$$\Phi^T(t) \{ (D_\phi^2)^T U + 2\alpha D_\phi^T U - UD_\phi^2 + \beta^2 U - K \} \Phi(x) = 0. \tag{31}$$

Using Eq. (19) in Eq. (31) we have

$$\Psi^T(t)G^T \{ (D_\phi^2)^T U + 2\alpha D_\phi^T U - UD_\phi^2 + \beta^2 U - K \} G\Psi(x) = 0. \tag{32}$$

Because of the independency between the entries of vector Ψ , we get

$$H = G^T \{ (D_\phi^2)^T U + 2\alpha D_\phi^T U - UD_\phi^2 + \beta^2 U - K \} G = 0. \tag{33}$$

Eq. (33) gives $(2^{J+2} - 1) \times (2^{J+2} - 1)$ independent equations, because the rank of matrix D_ϕ is 2^{J+2} and the rank of D_ϕ^2 is $2^{J+2} - 1$. Here we choose the independent equations as

$$H_{i,j} = 0, \quad i, j = 2, \dots, 2^{J+2} - 1. \tag{34}$$

Using Eq. (13) we can approximate the functions $g_1(x)$, $g_2(x)$, $h_1(t)$ and $h_2(t)$ as

$$\begin{aligned} g_1(x) &= V_1^T \Psi(x), \\ g_2(x) &= V_2^T \Psi(x), \\ h_1(t) &= V_3^T \Psi(t), \\ h_2(t) &= V_4^T \Psi(t), \end{aligned} \tag{35}$$

where V_1, V_2, V_3 and V_4 are vectors of dimension 2^{J+2} , and can be found using Eq. (15). Applying Eqs. (25), (26) and (35) in the initial and boundary conditions (3) – (6) we get

$$\begin{aligned} \Psi^T(0)U\Psi(x) &= V_1^T \Psi(x), \\ \Psi^T(0)D_\psi^T U\Psi(x) &= V_2^T \Psi(x), \\ \Psi^T(t)U\Psi(0) &= \Psi^T(t)V_3, \\ \Psi^T(t)U\Psi(2\pi) &= \Psi^T(t)V_4. \end{aligned} \tag{36}$$

The entries of vectors $\Psi(t)$ and $\Psi(x)$ are independent, so Eq.(36) gives

$$\begin{aligned} \Psi^T(0)U &= V_1^T, \\ \Psi^T(0)D_\psi^T U &= V_2^T, \\ U\Psi(0) &= V_3, \\ U\Psi(2\pi) &= V_4. \end{aligned} \tag{37}$$

Let

$$\begin{aligned} \Lambda_1 &= \Psi^T(0)U - V_1^T, \\ \Lambda_2 &= \Psi^T(0)D_\psi^T U - V_2^T, \\ \Lambda_3 &= U\Psi(0) - V_3, \\ \Lambda_4 &= U\Psi(2\pi) - V_4. \end{aligned} \tag{38}$$

By choosing the first 2^{J+2} equations of any equations $\Lambda_1 = 0, \Lambda_2 = 0, \Lambda_3 = 0$ and $\Lambda_4 = 0$ we get 2^{J+4} equations, mean

$$\begin{aligned} \Lambda_{1i} &= 0, \quad i = 1, 2, \dots, 2^{J+2}, \\ \Lambda_{2i} &= 0, \quad i = 1, 2, \dots, 2^{J+2}, \\ \Lambda_{3i} &= 0, \quad i = 1, 2, \dots, 2^{J+2}, \\ \Lambda_{4i} &= 0, \quad i = 1, 2, \dots, 2^{J+2}. \end{aligned} \tag{39}$$

Eq. (34) together with Eq. (39) gives 2^{2J+4} equations, which can be solved for $U_{i,j}, i, j = 1, 2, \dots, 2^{J+2}$. So the unknown function $u(x, t)$ can be found.

4. CONVERGENCE ANALYSIS OF TRIGONOMETRIC WAVELET METHOD

Now we shall give the error analysis of the method presented in the previous section for the telegraph equation (1).

Lemma 4.1. (see Chui [24], Dahmen et all. [26]) For any $J \in \mathbb{N}_0$, The interpolation operator P_J mapping any real-valued differentiable 2π -periodic function f into the space V_J is defined as follows

$$P_J f(x) = \sum_{k=0}^{2^{J+1}-1} [f(x_{J,k})\phi_{J,k}^0(x) + f'(x_{J,k})\phi_{J,k}^1(x)].$$

The following properties of the operators P_J are therefore obvious :

- i) $P_J f \in T_{2^{J+1}}$,
- ii) $P_J f(x_{J,k}) = f(x_{J,k})$ and $(P_J f)'(x_{J,k}) = f'(x_{J,k})$, $k \in \mathbb{Z}$,
- iii) $P_J f = f$ for all $f \in V_J$.

Lemma 4.2. (*L_p -Bernstein Inequality Lorentz and Lorentz [17, 18]*) Let f belong to trigonometric polynomial T_n of degree $\leq n$ then for we have

$$\|f'\|_p \leq n\|f\|_p, \quad 1 \leq p \leq \infty. \tag{40}$$

Theorem 4.3. (see Gao and Jang [10]) Assume that $k(x, t) \in L^2_{2\pi \otimes 2\pi}$, and its trigonometric wavelet approximation is $P_J k$, then it follows that

$$\|k(x, t) - P_J k(x, t)\|_{L^2_{2\pi \otimes 2\pi}} \leq C2^{-2(J+1)}, \tag{41}$$

where C is a positive constant value.

For the operator equation (1) the approximate equation is

$$P_J(\mathcal{A})u_J = P_J(\mathcal{D}_t - \mathcal{D}_x + \beta^2 \mathcal{I})u_J = f_J. \tag{42}$$

System (42) may be solved numerically to yield an approximate solution to (1) given by the expression $u_J = \Psi^T(t)U\Psi(x)$ and $f_J = \Psi^T(t)K\Psi(x)$.

At the first, we give the approximation results of the differential operators.

Theorem 4.4. Assume that $u(x, t) \in L^2_{2\pi \otimes 2\pi}$, and u is real-valued two time differentiable 2π -periodic function, then we have

$$\|\mathcal{D}_t u - P_J \mathcal{D}_t u\|_{L^2_{2\pi \otimes 2\pi}} \leq C \frac{J^2 + 2\alpha J}{2^{2(J+1)}}, \tag{43}$$

where C is a positive constant value. So $\|\mathcal{D}_t u - P_J \mathcal{D}_t u\|_{L^2_{2\pi \otimes 2\pi}} \rightarrow 0$, when $J \rightarrow \infty$.

Proof. Because the trigonometric wavelets belong to the trigonometric polynomial, using (40) and (41), we have

$$\begin{aligned} \|\mathcal{D}_t u - P_J \mathcal{D}_t u\|_{L^2_{2\pi \otimes 2\pi}} &\leq \|u_{tt} + 2\alpha u_t - P_J u_{tt} - 2\alpha P_J u_t\|_{L^2_{2\pi \otimes 2\pi}} \\ &\leq \|u_{tt} - P_J u_{tt}\|_{L^2_{2\pi \otimes 2\pi}} + 2\alpha \|u_t - P_J u_t\|_{L^2_{2\pi \otimes 2\pi}} \\ &\leq \|(u - P_J u)_{tt}\|_{L^2_{2\pi \otimes 2\pi}} + 2\alpha \|(u - P_J u)_t\|_{L^2_{2\pi \otimes 2\pi}} \\ &\leq J^2 \|u - P_J u\|_{L^2_{2\pi \otimes 2\pi}} + 2\alpha J \|u - P_J u\|_{L^2_{2\pi \otimes 2\pi}} \\ &\leq C(J^2 + 2\alpha J)2^{-2(J+1)}. \end{aligned}$$

□

Theorem 4.5. Assume that $u(x, t) \in L^2_{2\pi \otimes 2\pi}$, and u is real-valued two time differentiable 2π -periodic function, then we have

$$\|\mathcal{D}_x u - P_J \mathcal{D}_x u\|_{L^2_{2\pi \otimes 2\pi}} \leq C \frac{J^2}{2^{2(J+1)}}, \tag{44}$$

where C is a positive constant value. So $\|\mathcal{D}_x u - P_J \mathcal{D}_x u\|_{L^2_{2\pi \otimes 2\pi}} \rightarrow 0$, when $J \rightarrow \infty$.

Proof. The proof is similar to the proof of theorem 4.4. □

Next, the error $e_J = u - u_J$ of the approximate solution will be presented.

Theorem 4.6. Assume that u_J is the approximate solution of (1), the exact solution of (1) is u , also the operator $\mathcal{A} = \mathcal{D}_t - \mathcal{D}_x + \beta^2 \mathcal{I}$ has bounded inverse and $u(x, t), f(x, t) \in L^2_{2\pi \otimes 2\pi}$, are real-valued two time differentiable 2π -periodic functions, then we have

$$\|e_J\|_{L^2_{2\pi \otimes 2\pi}} \leq C(2J^2 + 2\alpha J + \beta^2 + 1)2^{-2(J+1)}. \tag{45}$$

Proof. Subtracting Eq. (42) from (1) yields

$$-P_J \mathcal{A}(u - u_J) = (\mathcal{A} - P_J \mathcal{A})u - (f - f_J),$$

provided that \mathcal{A}^{-1} exists, we obtain the error bound

$$\|e_J\|_{L^2_{2\pi \otimes 2\pi}} = \|(P_J \mathcal{A})^{-1}\|_{L^2_{2\pi \otimes 2\pi}} \|(\mathcal{A} - P_J \mathcal{A})u - (f - f_J)\|_{L^2_{2\pi \otimes 2\pi}}.$$

Furthermore, by using theorems 4.3-4.5, we have

$$\begin{aligned} \|(\mathcal{A} - P_J \mathcal{A})u\|_{L^2_{2\pi \otimes 2\pi}} &\leq \|(\mathcal{D}_t - P_J \mathcal{D}_t)u\|_{L^2_{2\pi \otimes 2\pi}} + \|(\mathcal{D}_x - P_J \mathcal{D}_x)u\|_{L^2_{2\pi \otimes 2\pi}} + \beta^2 \|(\mathcal{I} - P_J \mathcal{I})u\|_{L^2_{2\pi \otimes 2\pi}} \\ &\leq C_1 2^{-2(J+1)}(2J^2 + 2\alpha J + \beta^2), \end{aligned}$$

and

$$\|f - f_J\|_{L^2_{2\pi \otimes 2\pi}} \leq C_2 2^{-2(J+1)}.$$

From [11, p.142], we know that $P_J \mathcal{A}$ is invertible for large J , and its inverse has the same bound. Therefore, we get

$$\|u - u_J\|_{L^2_{2\pi \otimes 2\pi}} \leq C(2J^2 + 2\alpha J + \beta^2 + 1)2^{-2(J+1)},$$

where $C \geq \max\{C_1, C_2\}$. □

Remark. It was discovered in [1, 25] that the representation of an integral operator by compactly supported orthonormal wavelets produces numerically sparse matrices to some degree of precision. The properties of trigonometric wavelet base determine that the trigonometric wavelet compression technique cannot be applied well compared with the other wavelet methods [4, 23]. In this problem we see that the matrix of coefficients of the obtained system is a sparse matrix. In following examples we see that the percentage of sparsity for $J = 1$ is 91.58 and for $J = 2$ is 96.04. This can reduce the whole computational cost and facilitate the iterative method for the resulting algebraic equation. Figures 1, 2 show the plots of sparsity using the method proposed in this paper.

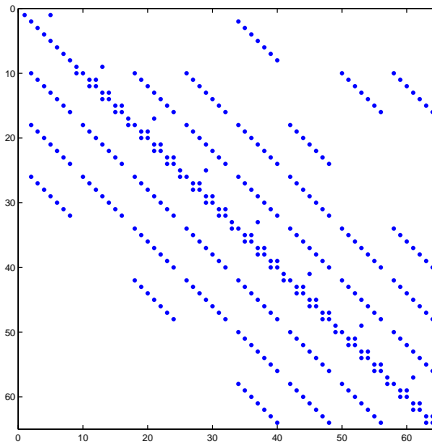


Fig. 1. Plot of sparsity with percentage of 91.58% for $J=1$.

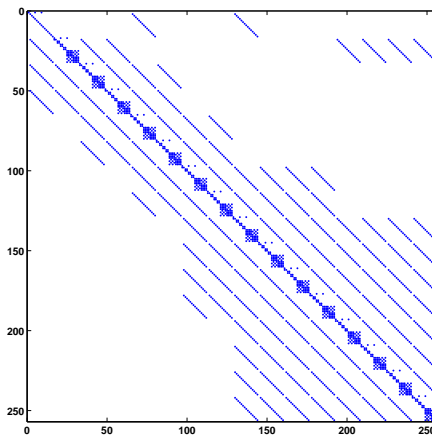


Fig. 2. Plot of sparsity with percentage of 96.04% for $J=2$.

$\tau=0.5$	$\alpha=20,$	$\beta=10$	$\alpha=10,$	$\beta=5$
J	TWM	CCFM	TWM	CCFM
0	3.5×10^{-11}	3.2×10^{-7}	5.0×10^{-11}	3.6×10^{-7}
1	2.3×10^{-15}	2.0×10^{-10}	4.4×10^{-14}	4.1×10^{-10}
2	5.0×10^{-17}	2.3×10^{-13}	3.5×10^{-18}	3.5×10^{-13}
3	3.1×10^{-21}	1.1×10^{-16}	5.6×10^{-21}	3.4×10^{-16}

Tab. 1. RMS errors.

$\tau=1.0$	$\alpha=20,$	$\beta=10$	$\alpha=10,$	$\beta=5$
J	TWM	CCFM	TWM	CCFM
0	1.1×10^{-11}	3.4×10^{-6}	2.1×10^{-11}	2.1×10^{-6}
1	5.4×10^{-14}	3.7×10^{-9}	1.2×10^{-13}	2.1×10^{-9}
2	2.7×10^{-16}	2.4×10^{-12}	3.7×10^{-17}	1.4×10^{-12}
3	7.8×10^{-21}	1.0×10^{-15}	3.7×10^{-21}	6.5×10^{-16}

Tab. 2. RMS errors.

5. ILLUSTRATIVE EXAMPLES

To support our theoretical discussion, we applied the method presented in this paper to several examples.

Example 5.1. Consider the equation (1.1) with the following conditions:

$$\begin{aligned}
 g_1(x) &= \sin(x), \\
 g_2(x) &= 0, \\
 h_1(t) &= 0, \\
 h_2(t) &= \cos(t) \sin(2\pi), \\
 f(x, t) &= -2\alpha \sin(t) \sin(x) + \beta^2 \cos(t) \sin(x).
 \end{aligned}$$

The exact solution is given by [9, 14, 22]

$$u(x, t) = \cos(t) \sin(x).$$

In this example we calculate the RMS error by the following formula

$$\text{RMS error} = \sqrt{\frac{\sum_{m=0}^{2^{j+2}-1} (u(x_{j,m}, \tau) - \hat{u}(x_{j,m}, \tau))^2}{2^{j+2}}},$$

where u and \hat{u} are the exact and approximate solution of the problem, respectively and τ is an arbitrary time t in $[0, 2\pi]$. In Tables 1 and 2 we represent the RMS errors obtained by Trigonometric wavelet method (TWM) in comparison with Chebyshev cardinal functions method (CCFM) [9]. The space-time graph of the numerical solution and error graph for $t \in [0, 2\pi]$ and $x \in [0, 2\pi]$ are presented in Figure 3.

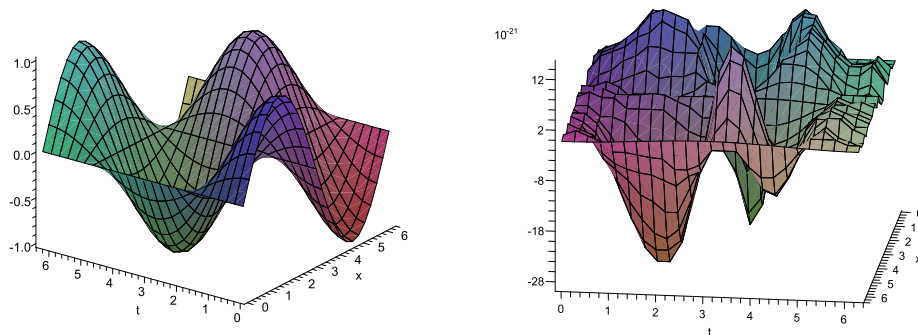


Fig. 3. Space-time graph of the estimated solution (left) and error graph (right) with $\alpha = 20$, $\beta = 10$ and $J=3$, for example 1.

Example 5.2. As the second test problem, Consider the equation (1.1) with the following conditions:

$$\begin{aligned}
 g_1(x) &= e^{\sin x}, \\
 g_2(x) &= \cos(x)e^{\sin x}, \\
 h_1(t) &= e^{\sin t}, \\
 h_2(t) &= e^{\sin(2\pi+t)}, \\
 f(x, t) &= (2\alpha \cos(x + t) + \beta^2)e^{\sin(x+t)}.
 \end{aligned}$$

The exact solution is given by

$$u(x, t) = e^{\sin(x+t)}.$$

Tables 3 and 4 show the absolute error using the technique presented in this paper with $J=2,3$ and different values of α , and β . The space-time graph of the numerical solution and error graph for $t \in [0, 2\pi]$ and $x \in [0, 2\pi]$ are presented in Figure 4.

Example 5.3. Consider the equation (1.1) with the following conditions:

$$\begin{aligned}
 g_1(x) &= \sin(x)\ln(2\pi + 1), \\
 g_2(x) &= 0, \\
 h_1(t) &= 0, \\
 h_2(t) &= 0, \\
 f(x, t) &= \sin x \left(\frac{-2\pi-1}{(\cos t+2\pi)^2} - \frac{2\alpha \sin t}{\cos t+2\pi} + (\beta^2 + 1)\ln(\cos t + 2\pi) \right).
 \end{aligned}$$

The exact solution is given by

$$u(x, t) = \sin(x)\ln(\cos t + 2\pi).$$

x	$\alpha=20,$	$\beta=10$	$\alpha=10,$	$\beta=5$
	$t = 1$	$t = 2$	$t = 1$	$t = 2$
0	2.49×10^{-7}	3.40×10^{-7}	2.49×10^{-7}	4.30×10^{-6}
$2\pi/9$	6.85×10^{-7}	8.22×10^{-7}	1.10×10^{-6}	1.52×10^{-6}
$4\pi/9$	7.12×10^{-7}	7.17×10^{-7}	1.19×10^{-6}	1.53×10^{-6}
$6\pi/9$	6.00×10^{-7}	4.52×10^{-7}	1.03×10^{-6}	1.20×10^{-6}
$8\pi/9$	4.31×10^{-7}	2.07×10^{-7}	8.36×10^{-7}	9.48×10^{-7}
$10\pi/9$	3.56×10^{-7}	1.71×10^{-7}	7.53×10^{-7}	9.52×10^{-7}
$12\pi/9$	4.25×10^{-7}	3.81×10^{-7}	8.45×10^{-7}	1.25×10^{-6}
$14\pi/9$	5.61×10^{-7}	6.80×10^{-7}	1.02×10^{-6}	1.64×10^{-6}
$16\pi/9$	6.34×10^{-7}	8.30×10^{-7}	1.05×10^{-6}	1.64×10^{-6}
2π	2.49×10^{-7}	4.30×10^{-7}	2.49×10^{-7}	4.30×10^{-7}

Tab. 3. Absolute values of errors for $u(x, t)$ with $J = 2$.

x	$\alpha=20,$	$\beta=10$	$\alpha=10,$	$\beta=5$
	$t = 1$	$t = 2$	$t = 1$	$t = 2$
0	3.04×10^{-18}	2.58×10^{-19}	3.04×10^{-18}	2.58×10^{-19}
$2\pi/9$	1.34×10^{-17}	2.59×10^{-17}	2.33×10^{-17}	3.43×10^{-17}
$4\pi/9$	1.21×10^{-17}	2.19×10^{-17}	2.25×10^{-17}	3.62×10^{-17}
$6\pi/9$	1.21×10^{-17}	1.98×10^{-17}	2.21×10^{-17}	3.36×10^{-17}
$8\pi/9$	1.32×10^{-17}	1.77×10^{-17}	2.28×10^{-17}	3.12×10^{-17}
$10\pi/9$	1.30×10^{-17}	1.77×10^{-17}	2.25×10^{-17}	3.16×10^{-17}
$12\pi/9$	1.10×10^{-17}	1.94×10^{-17}	2.09×10^{-17}	3.42×10^{-17}
$14\pi/9$	1.56×10^{-17}	2.12×10^{-17}	2.09×10^{-17}	3.66×10^{-17}
$16\pi/9$	1.27×10^{-17}	2.58×10^{-17}	2.23×10^{-17}	3.49×10^{-17}
2π	3.04×10^{-18}	2.58×10^{-19}	3.04×10^{-18}	2.58×10^{-19}

Tab. 4. Absolute values of errors for $u(x, t)$ with $J = 3$.

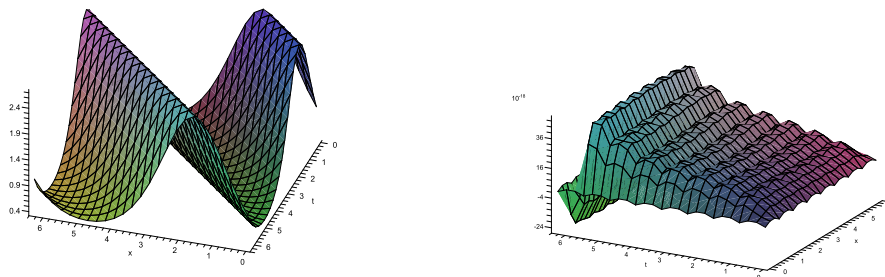


Fig. 4. Space-time graph of the estimated solution (left) and error graph (right) with $\alpha = 20$, $\beta = 10$ and $J=3$, for example 2.

Tables 5 and 6 show the absolute error using the technique presented in this paper with $J=2,3$ and different values of α , and β . The space-time graph of the numerical solution and error for $t \in [0, 2\pi]$ and $x \in [0, 2\pi]$ are presented in Figure 5.

Example 5.4. Consider the equation (1.1) with the following conditions:

$$\begin{aligned}
 g_1(x) &= 0, \\
 g_2(x) &= \frac{2}{2 + \cos(x)}, \\
 h_1(t) &= \frac{\sin(2t)}{3}, \\
 h_2(t) &= \frac{\sin(2t)}{3}, \\
 f(x, t) &= -\frac{2 \sin(2t) \sin^2(x)}{(2 + \cos(x))^3} - \frac{\sin(2t) \cos(x)}{(2 + \cos(x))^2} + \frac{(\beta^2 - 4) \sin(2t) + 4\alpha \cos(2t)}{2 + \cos(x)}.
 \end{aligned}$$

The exact solution is given by

$$u(x, t) = \frac{\sin(2t)}{2 + \cos(x)}.$$

Tables 7 and 8 show the absolute error using the technique presented in this paper with $J=2,3$ and different values of α , and β . The space-time graph of the numerical solution and error for $t \in [0, 2\pi]$ and $x \in [0, 2\pi]$ are presented in Figure 6.

x	$\alpha=20,$ $t = 1$	$\beta=10$ $t = 2$	$\alpha=10,$ $t = 1$	$\beta=5$ $t = 2$
0	2.50×10^{-10}	1.41×10^{-9}	1.08×10^{-11}	1.46×10^{-10}
$2\pi/9$	1.21×10^{-9}	3.35×10^{-9}	1.38×10^{-10}	8.42×10^{-9}
$4\pi/9$	1.85×10^{-9}	5.14×10^{-9}	2.11×10^{-10}	1.29×10^{-8}
$6\pi/9$	1.63×10^{-9}	4.52×10^{-9}	1.86×10^{-10}	1.13×10^{-8}
$8\pi/9$	6.44×10^{-10}	1.74×10^{-9}	7.35×10^{-11}	4.48×10^{-9}
$10\pi/9$	6.44×10^{-10}	1.78×10^{-9}	7.35×10^{-11}	4.48×10^{-9}
$12\pi/9$	1.63×10^{-9}	4.52×10^{-9}	1.86×10^{-10}	1.13×10^{-8}
$14\pi/9$	1.85×10^{-9}	5.14×10^{-9}	2.11×10^{-10}	1.29×10^{-8}
$16\pi/9$	1.21×10^{-9}	3.35×10^{-9}	1.38×10^{-10}	8.42×10^{-9}
2π	2.50×10^{-10}	1.41×10^{-9}	1.08×10^{-11}	1.46×10^{-10}

Tab. 5. Absolute values of errors for $u(x, t)$ with $J = 2$.

x	$\alpha=20,$ $t = 1$	$\beta=10$ $t = 2$	$\alpha=10,$ $t = 1$	$\beta=5$ $t = 2$
0	3.00×10^{-20}	1.00×10^{-20}	9.03×10^{-21}	5.35×10^{-20}
$2\pi/9$	6.54×10^{-18}	7.10×10^{-18}	6.01×10^{-18}	2.11×10^{-17}
$4\pi/9$	1.04×10^{-17}	1.03×10^{-17}	8.31×10^{-18}	3.27×10^{-17}
$6\pi/9$	9.33×10^{-18}	9.13×10^{-18}	7.84×10^{-18}	2.99×10^{-17}
$8\pi/9$	3.52×10^{-18}	3.79×10^{-18}	2.77×10^{-18}	1.05×10^{-17}
$10\pi/9$	3.72×10^{-18}	3.99×10^{-18}	3.06×10^{-18}	1.12×10^{-17}
$12\pi/9$	8.70×10^{-18}	8.89×10^{-18}	7.39×10^{-18}	2.83×10^{-17}
$14\pi/9$	1.00×10^{-17}	1.04×10^{-17}	8.80×10^{-18}	3.43×10^{-17}
$16\pi/9$	6.24×10^{-18}	6.67×10^{-18}	5.04×10^{-18}	2.20×10^{-17}
2π	3.00×10^{-20}	1.00×10^{-20}	9.03×10^{-21}	5.35×10^{-20}

Tab. 6. Absolute values of errors for $u(x, t)$ with $J = 3$.

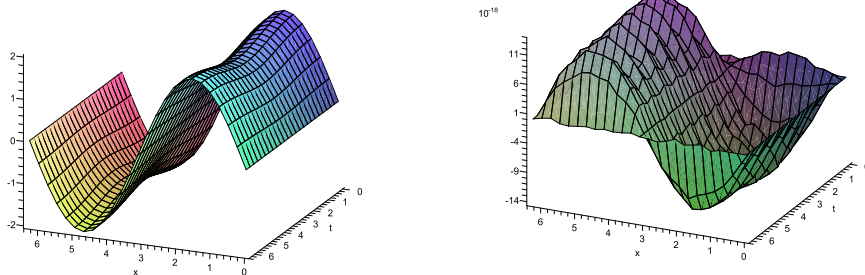


Fig. 5. Space-time graph of the estimated solution (left) and error graph (right) with $\alpha = 20$, $\beta = 10$ and $J=3$, for example 3.

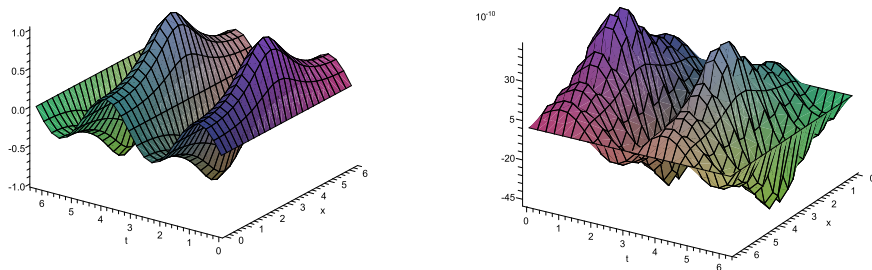


Fig. 6. Space-time graph of the estimated solution (left) and error graph (right) with $\alpha = 20$, $\beta = 10$ and $J=3$, for example 4.

6. CONCLUSION

The trigonometric wavelets are used to solve the telegraph equation. Some properties of trigonometric wavelets are presented and the operational matrices of derivative for trigonometric scaling functions and wavelets are utilized to reduce the solution of telegraph equation to the solution of linear system of equations with sparse matrix of coefficients. The trigonometric Hermite interpolant wavelet method in this paper tackles this difficulty of the large costs of computation and transforms the dense matrix due to its simple explicit forms. The convergence analysis is developed. The method is computationally attractive and applications are demonstrated through illustrative examples.

x	$\alpha=20,$	$\beta=10$	$\alpha=10,$	$\beta=5$
	$t = 1$	$t = 2$	$t = 1$	$t = 2$
0	9.02×10^{-21}	7.56×10^{-21}	9.09×10^{-21}	7.56×10^{-21}
$2\pi/9$	1.41×10^{-5}	4.82×10^{-6}	3.85×10^{-5}	3.81×10^{-6}
$4\pi/9$	3.58×10^{-5}	1.64×10^{-5}	6.66×10^{-5}	8.33×10^{-7}
$6\pi/9$	6.78×10^{-5}	4.19×10^{-5}	1.24×10^{-4}	1.45×10^{-5}
$8\pi/9$	1.23×10^{-4}	7.79×10^{-5}	2.14×10^{-4}	4.00×10^{-5}
$10\pi/9$	1.23×10^{-4}	7.79×10^{-5}	2.14×10^{-4}	4.00×10^{-5}
$12\pi/9$	6.78×10^{-5}	4.19×10^{-5}	1.24×10^{-4}	1.45×10^{-5}
$14\pi/9$	3.58×10^{-5}	1.64×10^{-5}	6.66×10^{-5}	8.33×10^{-7}
$16\pi/9$	1.41×10^{-5}	4.82×10^{-6}	3.85×10^{-5}	3.81×10^{-6}
2π	9.02×10^{-21}	7.56×10^{-21}	9.09×10^{-21}	7.56×10^{-21}

Tab. 7. Absolute values of errors for $u(x, t)$ with $J = 2$.

x	$\alpha=20,$	$\beta=10$	$\alpha=10,$	$\beta=5$
	$t = 1$	$t = 2$	$t = 1$	$t = 2$
0	5.60×10^{-21}	1.01×10^{-20}	9.00×10^{-21}	2.31×10^{-20}
$2\pi/9$	1.46×10^{-9}	4.58×10^{-10}	4.48×10^{-9}	7.14×10^{-10}
$4\pi/9$	2.56×10^{-9}	1.11×10^{-9}	6.80×10^{-9}	7.58×10^{-10}
$6\pi/9$	3.53×10^{-9}	1.36×10^{-9}	9.97×10^{-9}	1.41×10^{-9}
$8\pi/9$	3.53×10^{-9}	6.51×10^{-10}	1.27×10^{-8}	3.16×10^{-9}
$10\pi/9$	3.53×10^{-9}	6.51×10^{-10}	1.27×10^{-8}	3.16×10^{-9}
$12\pi/9$	3.53×10^{-9}	1.36×10^{-9}	9.97×10^{-9}	1.41×10^{-9}
$14\pi/9$	2.56×10^{-9}	1.11×10^{-9}	6.80×10^{-9}	7.58×10^{-10}
$16\pi/9$	1.46×10^{-9}	4.58×10^{-10}	4.48×10^{-9}	7.14×10^{-10}
2π	5.60×10^{-21}	1.01×10^{-20}	9.00×10^{-21}	2.31×10^{-20}

Tab. 8. Absolute values of errors for $u(x, t)$ with $J = 3$.

ACKNOWLEDGEMENT

The authors are very grateful to both referees for carefully reading the paper and for comments and suggestions which have improved the paper.

(Received October 26, 2011)

REFERENCES

-
- [1] B. Alpert, G. Beylkin, R. Coifman, and V. Rokhlin: Wavelet-like bases for the fast solution of second-kind integral equation. *SIAM J. Sci. Comput.* *14* (1993), 159–184.
 - [2] C.K. Chui and H.N. Mhaskar: On trigonometric wavelets. *Constr. Approx.* *9* (1993), 167–190.
 - [3] C.K. Chui: *An Introduction to Wavelets*. Academic Press, Boston 1992.
 - [4] W. Dahmen, S. Prössdorf, and R. Schneider: Wavelet approximation methods for pseudodifferential equations. In: *Stability and Convergence*, *Math. Z.* *215* (1994), 583–620.
 - [5] M. Dehghan: On the solution of an initial-boundary value problem that combines Neumann and integral condition for the wave equation. *Numer. Methods Partial Differential Equations* *21* (2005), 24–40.
 - [6] M. Dehghan: Finite difference procedures for solving a problem arising in modeling and design of certain optoelectronic devices. *Math. Comput. Simulation* *71* (2006), 16–30.
 - [7] M. Dehghan: Implicit collocation technique for heat equation with non-classic initial condition. *Internat. J. Non-Linear Sci. Numer. Simul.* *7* (2006), 447–450.
 - [8] M. Dehghan and A. Shokri: A numerical method for solving the hyperbolic telegraph equation. *Numer. Methods Partial Differential Equations* *24* (2008), 1080–1093.
 - [9] M. Dehghan and M. Lakestani: The use of Chebyshev cardinal functions for solution of the second-order one-dimensional telegraph equation. *Numer. Methods Partial Differential Equations* *25* (2009), 931–938.
 - [10] J. Gao and Y.L. Jiang: Trigonometric Hermite wavelet approximation for the integral equations of second kind with weakly singular kernel. *J. Comput. Appl. Math.* *215* (2008), 242–259.
 - [11] R. Kress: *Linear Integral Equations*. Springer, New York 1989.
 - [12] M. Lakestani and M. Dehghan: The solution of a second-order nonlinear differential equation with Neumann boundary conditions using semi-orthogonal B-spline wavelets. *Internat. J. Comput. Math.* *83* (2006), 8–9, 685–694.
 - [13] M. Lakestani, M. Razzaghi, and M. Dehghan: Semiorthogonal wavelets approximation for Fredholm integro-differential equations. *Math. Prob. Engrg.* (2006), 1–12.
 - [14] M. Lakestani and B.N. Saray: Numerical solution of telegraph equation using interpolating scaling functions. *Comput. Math. Appl.* *60* (2010), 7, 1964–1972.
 - [15] M. Lakestani, M. Jokar, and M. Dehghan: Numerical solution of nth-Order Integro-Differential equations using trigonometric wavelets. *Numer. Math. Methods Appl. Sci.* *34* (2011), 11, 1317–1329.
 - [16] L. Lapidus and G.F. Pinder,: *Numerical Solution of Partial Differential Equations in Science and Engineering*. Wiley, New York 1982.
 - [17] G.G. Lorentz: Convergence theorems for polynomials with many zeros. *Math. Z.* *186* (1984), 117–123.
 - [18] G.G. Lorentz and R.A. Lorentz: *Mathematics from Leningrad to Austin*. In: *Selected Works In Real, Functional And Numerical Analysis*, (1997).
 - [19] R.K. Mohanty, M.K. Jain, and K. George: On the use of high order difference methods for the system of one space second order non-linear hyperbolic equations with variable coefficients. *J. Comput. Appl. Math.* *72* (1996), 421–431.

- [20] R. K. Mohanty: An unconditionally stable difference scheme for the one-space dimensional linear hyperbolic equation. *Appl. Math. Lett.* *17* (2004), 101–105.
- [21] R. K. Mohanty: An unconditionally stable finite difference formula for a linear second order one space dimensional hyperbolic equation with variable coefficients. *Appl. Math. Comput.* *165* (2005), 229–236.
- [22] A. Mohebbi and M. Dehghan: High order compact solution of the one-space-dimensional linear hyperbolic equation. *Numer. Methods Partial Differential Equations* *24* (2008), 1222–1235.
- [23] T. V. Petersdorff and C. Schwab: Wavelet approximation for first kind integral equations on polygons. *Numer. Math.* *74* (1996), 479–516.
- [24] E. Quak: Trigonometric wavelets for hermite interpolation. *J. Math. Comput.* *65* (1996), 683–722.
- [25] M. Shamsi and M. Razzaghi: Solution of Hallen’s integral equation using multiwavelets. *Comput. Phys. Comm.* *168* (2005), 187–197.
- [26] Z. Shan and Q. Du: Trigonometric wavelet method for some elliptic boundary value problems. *J. Math. Anal. Appl.* *344* (2008), 1105–1119.
- [27] E. H. Twizell: An explicit difference method for the wave equation with extended stability range. *BIT* *19* (1979), 378–383.

Mahmood Jokar, Department of Applied Mathematics, Faculty of Mathematical Sciences, University of Tabriz, Tabriz. Iran.

e-mail: jokar.mahmod@gmail.com

Mehrdad Lakestani, Department of Applied Mathematics, Faculty of Mathematical Sciences, University of Tabriz, Tabriz. Iran.

e-mail: lakestani@tabrizu.ac.ir